Applied Thermal Engineering 279 (2025) 127901

Contents lists available at ScienceDirect

Applied Thermal Engineering

journal homepage: www.elsevier.com/locate/apthermeng

Research Paper

Thermo-economic investigation and multi objective optimization of cascade high temperature heat pump using low global warming refrigerants

Duy K. Hoang [a], Timothy G. Walmsley [b], Don J. Cleland [c], Qun Chen [c], James K. Carson [b,*]

[a] Energy Efficiency and Conservation Authority, Wellington 6011, New Zealand
[b] Ahuora-Center for Smart Energy Systems, School of Engineering, The University of Waikato, Hamilton 3240, New Zealand
[c] School of Food Technology and Natural Sciences, Massey University, Palmerston North 4474, New Zealand

ARTICLE INFO

Keywords:
Heat pump
Cascade cycle
Differential evolution
Spray dryer

ABSTRACT

High temperature heat pumping (HTHP) is a key technology for decarbonizing industrial process heat. This paper describes an investigation into the thermodynamic and economic performance of a cascade HTHP configured with internal heat exchangers (IHXs), using low global warming potential (GWP) refrigerants in both the top cycle and the bottom cycle. The proposed system was applied to a spray dryer case study with supply air temperature over 200 °C. A differential evolution (DE) method was used to optimize operating parameters to obtain the maximum COP. The simulation results indicated that of the cycles and refrigerants considered, the maximum COP can be obtained when using acetone or ethanol in the top cycle (TC) and butane or neopentane in the bottom cycle (BC). The use of acetone/neopentane and ethanol/neopentane achieved a highest COP of 2.42; however, better economic performance was achieved when using butane as the BC refrigerant rather than neopentane, while the economic and thermodynamic performance of the heat pumps were similar when acetone and ethanol were used as TC refrigerants. The performance of the most promising refrigerants was analyzed under off-design conditions, with minimum and maximum COP being 2.19 and 2.82, respectively obtained with the sink inlet/outlet temperature of 50 °C/230 °C and 15 °C/200 °C.

1. Introduction

Process heat accounted for 28 % of all energy related greenhouse gas emissions in New Zealand, in 2016, making it the second-largest contributor to emissions behind transport in the energy sector [1] (MBIE, 2017). As 56 % of all process heating demand was supplied by fossil fuels, the New Zealand Government has begun the implementation of a regulatory strategy to phase out fossil fuels and become carbon neutral by 2050. However, transitioning away from fossil fuels presents significant challenges. For example, low-cost biomass is predicted to only supply 22 % of process heat currently produced from combustion of fossil fuels [2] (Hall, 2017), while electrode boilers and hydrogen technologies are costly to operate.

High temperature heat pumping technology (HTHP) technology offers low-emission options for process heat suitable for a range of industries and is much more energy efficient than direct electrode or ohmic heating [3] (Arpagaus et al., 2016). In New Zealand, a significant portion of process heat is required at temperatures up to 200 °C and higher. There are several studies on HTHP for industrial processes which suggest sink output temperatures of approximately 200 °C may be achieved [4,5] (Kim et al., 2021; Unterluggauer et al., 2023). However, these models typically require a high heat source temperature of around 90 °C, which is not commonly available in many industries thereby limiting their scope for application. There are a number of industries where an HTHP that can reach 200 °C from near ambient heat source temperature would be required. However, high temperature lifts (i.e. difference between heat sink and heat source temperatures) are associated with a high throttling loss and a high pressure ratio which increases the work of compression and reduces the efficiency of the compressor and hence the COP of the cycle [6] (Adamson et al. 2022). One solution is to make use of cascade cycles, which consist of two or more independently operated single-stage refrigeration systems. Cascade cycles are more efficient than equivalent single-stage cycles because the compression work is divided among multiple compressors (Mota-Babiloni et al., 2018) [7]. In addition, they provide greater flexibility in choosing different pure refrigerants for each stage to achieve optimal performance.

A range of refrigerants have been tested in the cascade HTHP systems to find the suitable refrigerant pairings. Mota-Babiloni et al. [7] (2018)

* Corresponding author.
E-mail address: james.carson@waikato.ac.nz (J.K. Carson).

https://doi.org/10.1016/j.applthermaleng.2025.127901
Received 21 December 2024; Received in revised form 21 June 2025; Accepted 13 August 2025
Available online 14 August 2025

Nomenclature

h	enthalpy (kJ kg^{-1})
$\dot{m}$	mass flow rate (kg s^{-1})
T	temperature (°C)
p	pressure (bar)
Q	heat flow (kW)
s	entropy (kJ kg^{-1} °C^{-1})
X	exergy (kJ kg^{-1})
W	work (kW)
η	efficiency

Subscript

bot	Bottom
cond	Condenser
eva	Evaporator
ex	Exergy
is	Isentropic
me	Mechanic
sat	saturation
top	Top
II	second law
SH1	superheat at IHX1
SH2	superheat at IHX2
o	dead state

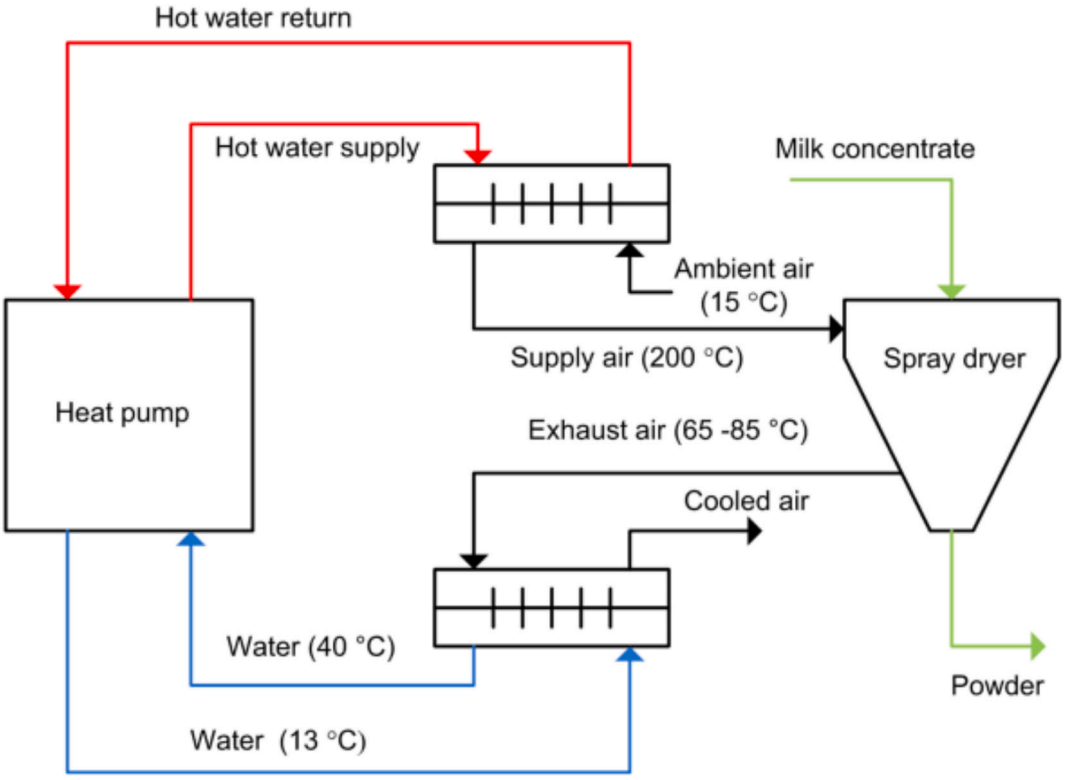

Fig. 1. Schematic of the spray dryer heat recovery using heat pump via water loops.

considered five different refrigerants for the low-stage and four different refrigerants for the high-stage in the two-stage cascade HTHP. The results indicated that the highest efficiency was obtained when butane and isobutane were used for the low-stage cycle and HFO-1336mzz(Z) and pentane were used for the high-stage cycle. They found that the high-stage refrigerant had a smaller influence on the system performance than the low-stage refrigerant. Using a theoretical analysis, [8] Li et al. (2019) compared six pairs of refrigerants for a water source cascade HTHP with the maximum sink outlet temperature varied from 100 °C to 170 °C. Their customized refrigerant BY3B/BY6 gave the highest COP, and the maximum hot water outlet temperature and temperature lift of the system using these refrigerants were 168.4 °C, and 113.4 °C, respectively. Uusitalo et al. [9] (2020) concluded that R601 and R245fa form the best refrigerant pairing for the low-stage and high-stage respectively of a cascade heat pump with a condensing temperature and evaporating temperature of 90 °C and 20 °C.

Dong et al. [10] (2024) and Dong and Wang [11] (2024) studied the performance of pairings of 15 refrigerants (2 HFC, 6 HFO, 2 HFCO 6 HC and ammonia) in four different cascade cycle designs. They concluded that HFO pairings provided the optimal working fluid combination when taking economics, thermodynamic efficiency and environmental factors into consideration. However, while HFOs and HFCOs do not have high GWP or ODP directly, the breakdown products can be quite harmful, and they may not receive long-term acceptance globally, given that they are already being phased out of Europe [12–14] (Song et al., 2024, Trevisan, 2023, EU, n.d.). Similarly, Hu et al. [15] (2024) studied the performance of a high temperature cascade system for waste heat recovery but employed HFCs R134a and R245fa that have high GWP and are being phased out in many jurisdictions.

Ganesan et al. [16] (2023) analyzed the performance of a cascade system using only natural refrigerants and natural refrigerant blends; however, they only obtained temperatures up to 118 °C; considerably

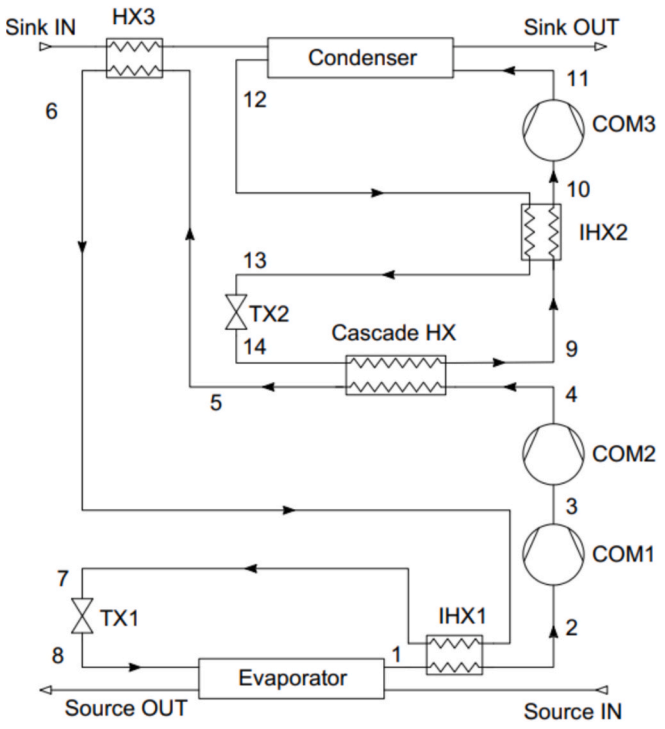

Fig. 2. Schematic diagram of the cascade heat pump cycle.

lower than the focus of this paper. Hosseinnia et al. [17] (2024) analyzed cascade systems with water in the high stage and a selection of refrigerants (three HFO and three HC) in the low stage. They concluded that with the aid of water injection in the high stage compressor sink temperatures as high as 190 °C could be achieved (lifting from a source temperature of 50 °C).

In addition to refrigerant selection, the performance of a cascade HTHP can be improved by optimizing the operating conditions. Mota-Babiloni et al. [7] (2018) performed optimization of the operating condition of a cascade HTHP configuration with internal heat exchangers (IHX) based on variation of the intermediate temperature and effectiveness of IHX. Zou et al. [18] (2020) used a Genetic Algorithm to optimize the intermediate temperature and vapor injection temperature of an air source cascade HTHP with vapor injection. A prototype cascade heat pump was built to verify the optimization method. The COP of the optimized prototype was 18.71 % higher than reported in the authors' previous study [19] (Zou et al., 2019) for a heat source temperature of 20 °C and heat sink temperature of 130 °C. Dong et al. [20] (2022) optimized the evaporation temperature and condensation temperature of a cascade HTHP using the cost per exergy output and initial cost per unit heat capacity as the objective functions. The results indicated that the optimal condensation temperature increased with the output water temperature while the optimal evaporation temperature was not significantly affected by the heat source temperature.

Despite many studies on cascade HTHP systems, there is none focused on systems with heat sink temperatures of 200 °C and above. Hence, the aim of this paper is to present and analyze a cascade HTHP system using low GWP refrigerants for applications at or above 200 °C. A multi-parameter optimization algorithm has been employed to optimize the operating conditions (including intermediate temperature and superheated temperature across IHXs) in both the bottom and top cycles for each refrigerant pairing. The scope of the analysis was limited to pure refrigerants in each stage, rather than refrigerant blends. Finally, an economic analysis was presented to evaluate the economic feasibility of the proposed cascade system for each refrigerant pair.

2. Context and proposed heat pump system

2.1. Operating conditions

In the New Zealand dairy industry, milk is spray dried using ambient air that is typically heated to about 200 °C producing an exhaust air temperature typically ranging between 65 and 85 °C [21] (Walmsley et al., 2015). In this study, a cascade HTHP was designed to integrate indirectly with spray dryers via water loops, as shown in Fig. 1. The cascade HTHP first heats pressurized water, which is then used to heat ambient air from 15 °C to 200 °C before it enters the spray dryer. A water loop between 13 °C and 40 °C which is preheated by spray dryer exhaust air was used as the heat source for the heat pump.

2.2. System description

The schematic diagram of the proposed two-stage cascade heat pump is presented in Fig. 2.

The heat pump includes a cascade heat exchanger, two internal heat exchangers (IHX1 and IHX2) one for each stage, and one heat exchanger (HX3) used to preheat the heat sink fluid by using the condensing heat from the bottom cycle (BC). To achieve an extremely high sink outlet temperature while maximize the use of condensing heat of the bottom cycle, two compressors in series were employed for the bottom cycle (in order that the pressure ratio in each may be limited to 8, while achieving the required temperature lift), while only one compressor was used for the top cycle (TC).

3. Methods

3.1. Thermodynamic model

The thermodynamic model of the system was implemented in Python using REFPROP v10 [22] (Lemmon et al., 2018) to obtain the thermodynamic properties of the refrigerant. The following assumptions were made when developing the heat pump model:

- Steady-state operation.
- No heat loss and pressure drop across the heat exchangers.
- Isenthalpic expansion.
- Isobaric heat transfer processes.
- Isentropic compression efficiency: $\eta_{is} = 70$ %.
- Compressor motor efficiency: $\eta_{me} = 96$ %.
- Internal heat exchangers: $\Delta T_{pinch,\ IHX} = 3$ °C.
- Heat sink (air): $\Delta T_{pinch,sink} = 20$ °C.
- Heat source (water): $\dot{Q}_{source} = 500$ kW, $\Delta T_{pinch,source} = 3$ °C.

In order to compare with other spray dryer air heating processes, air was used as heat sink indirectly via water loop, it was assumed that the minimum temperature difference between refrigerant and water was 5 °C, and the minimum temperature difference between water and air is 15 °C. Therefore, the minimum temperature difference between refrigerant and the air, $\Delta T_{pinch,sink}$, is 20 °C. Water was used as the heat source, with the minimum temperature different between refrigerant and water, $\Delta T_{pinch,source}$, of 3 °C. All heat exchangers were first subdivided into sub-cooling, evaporating/condensing, and superheating/de-superheating sections where the constant heat transfer coefficients presented in Table 2 were applied. Each section was then further divided into small control volumes to find the minimum temperature difference between the streams [23] (Zühlsdorf et al., 2018). The top cycle condensing pressure was determined using the Newton-Raphson method to set $\Delta T_{pinch,sink}$ to 20 °C. The evaporating temperature of the bottom cycle, $T_{eva,bot}$, was determined by subtracting, $\Delta T_{pinch,source}$ from the heat source outlet temperature. The evaporating pressure of the bottom cycle was then estimated from $T_{eva,\ bot}$ and the vapor quality of

Table 1
List of refrigerants considered for cascade HTHP with main characteristics.

	Refrigerant	ODP	GWP	Normal boiling point (°C)	P_{cr} (bar)	T_{cr} (°C)	Safety class
Bottom cycle (BC)	Butane	0	3.0	−0.8	38.0	152.0	A3
	Butene	–	–	−6.6	40.1	146.1	–
	cis-Butene	–	–	3.4	42.3	162.6	–
	Isobutane	0	3.0	−12.1	36.3	134.7	A3
	Isobutene	–	–	−7.3	40.1	144.94	–
	Neopentane	0	0	9.1	32.0	160.6	–
	R-1234ze(Z)	0	<10	9.4	–	150.1	A2L
Top cycle (TC)	Acetone	0	0.5	55.7	46.9	235.0	A3
	Benzene	0	low	79.6	49.1	288.9	A3
	Cyclohexane	0	low	80.3	40.8	280.5	A3
	Cyclopentane	0	<0.1	48.9	45.8	238.6	A3
	Ethanol	0	low	78.1	62.7	241.6	A3
	Heptane	0	3	98.0	27.4	267.1	A3
	Hexane	0	3	68.3	30.4	234.7	A3
	Isohexane	0	low	59.8	30.4	224.6	A3
	Isooctane	–	–	98.7	25.7	270.9	A3
	Methylcyclohexane	–	–	100.4	34.7	299.1	A3
	Toluene	0	3	110.1	41.3	318.6	B3

Table 2
Assumed heat transfer coefficients for heat exchanger area calculation [23,25] (Incropera et al., 2007; Zühlsdorf et al., 2018).

Flow condition	Heat transfer coefficient, W $m^{-2}K^{-1}$
Evaporation	3000
Condensation	2400
Liquid flow	1500
Gaseous flow	250

zero. The model assumed that the refrigerant left the bottom cycle evaporator as a superheated vapor with a temperature of 5C less than the heat source inlet.

The condensing temperature of the bottom cycle, defined as the intermediate temperature, T_{inter}, could be varied in the model. The evaporating temperature of the top cycle, $T_{eva,top}$, was determined by subtracting, ΔT_{pinch}, from the intermediate temperature. The temperature of the top cycle refrigerant leaving the cascade heat exchanger could be adjusted to maintain the minimum pinch point temperature difference in the cascade heat exchanger.

The increasing superheating temperatures (ΔT_{SH1}, ΔT_{SH2}) of the refrigerant across the internal heat exchangers (IHX1, and IHX2) could be varied in the model. The temperature differences at the hot liquid inlet of the IHXs were chosen to be equal to the ΔT_{pinch}.

Some simulations were run without IHX1 installed ($\Delta T_{SH1} = 0$), in which case the temperature of refrigerant leaving the HX3 could go as low as the sink inlet temperature plus $\Delta T_{pinch,sink.}$ However, it could be increased if the pinch point temperature difference of HX3 occured at the refrigerant inlet of the HX3.

Refrigerant entering HX3 at the intermediate temperature was assumed to be a saturated mixture with a vapor quality that could be varied in the model.

The thermodynamic states of the refrigerants at different points in the cycle were determined based on the energy balance equations for all components, as listed below. The subscript numbers refer to cycle locations in Fig. 2.

$$Evaporator: \quad \dot{Q}_{source} = \dot{m}_{source}\left(h_{source,IN} - h_{source,OUT}\right) = \dot{m}_{bot}\left(h_1 - h_8\right) \tag{1}$$

$$Condenser + HX3: \dot{Q}_{sink} = \dot{m}_{sink}\left(h_{sink,OUT} - h_{sink,IN}\right) = \dot{m}_{top}\left(h_{11} - h_{12}\right) + \dot{m}_{bot}\left(h_5 - h_6\right) \quad 2)$$

$$Compressor1: \dot{W}_1 = \frac{\dot{m}_{bot}\left(h_3 - h_2\right)}{\eta_{me}} h_3 = h_2 + \frac{h_{3is} - h_2}{\eta_{is}} \tag{3}$$

$$Compressor2: \dot{W}_2 = \frac{\dot{m}_{bot}\left(h_4 - h_3\right)}{\eta_{me}} h_4 = h_3 + \frac{h_{4is} - h_3}{\eta_{is}} \tag{4}$$

$$Compressor3: \dot{W}_3 = \frac{\dot{m}_{top}\left(h_{11} - h_{10}\right)}{\eta_{me}} h_{11} = h_{10} + \frac{h_{11is} - h_{10}}{\eta_{is}} \tag{5}$$

$$TX1: \quad h_7 = h_8 \tag{6}$$

$$TX2: \quad h_{13} = h_{14} \tag{7}$$

$$IHX1: \quad h_2 - h_1 = h_6 - h_7 \tag{8}$$

$$IHX2: \quad h_{10} - h_9 = h_{12} - h_{13} \tag{9}$$

$$CascadeHX: \quad \dot{m}_{bot}\left(h_4 - h_5\right) = \dot{m}_{top}\left(h_9 - h_{14}\right) \tag{10}$$

3.2. Refrigerant selection

This study only considers refrigerants with zero ozone depletion potential (ODP) and low global warming potential (GWP). Fukuda et al. [24] (2014) indicated that the theoretical COP of the HTHP is maximized when operating at a condensation temperature of approximately 20 °C below the critical temperature of the working fluid, and this criterion was also used to select refrigerants for consideration in this study. Refrigerants that would result in pressures lower than 1 atm in the evaporator of each cycle were excluded from consideration. Refrigerants that were considered for the top and bottom cycles are shown in Table 1.

Seven refrigerants were tested for the bottom cycle (BC), and eleven refrigerants were tested for top cycle (TC). Most refrigerants considered (except for R1234ze(Z)) are flammable (Safety class A3 or B3), and additional safety measures such as increased ventilation or gas detectors are required when handling them. However, for vapor compression systems located in a machinery room with access restricted to authorized personnel, there is no charge limitation for flammable refrigerants (EN 378–1:2017, 2017). Each BC refrigerant was paired with each TC in the simulations (i.e. 77 refrigerant pairings were tested).

3.3. Thermal performance evaluation

The thermodynamic performance of the heat pump cycle can be analyzed based on different indicators. The COP relates the useful heat flow to the consumed electric power of the compressors:

$$COP = \frac{\dot{Q}_{sink}}{\dot{W}_1 + \dot{W}_2 + \dot{W}_3} \tag{11}$$

Table 3
Parameters for economic evaluation.

Parameter	Value	Reference
Specific cost of electricity, c_{el}	146.6 NZD/MWh	[28] (MBIE, 2022)
Specific cost of natural gas, c_{NG}	51.6 NZD/MWh	[28] (MBIE, 2022)
Emission factor of electricity, E_{el}	107 kg CO2/MWh	[29] (MfE, 2022)
Emission factor of natural gas, E_{NG}	195 kg CO2/MWh	[29] (MfE, 2022)
Carbon price, c_{carbon}	80.25 NZD/ton of CO2	[30] (Carbonnews, 2023)
Annual operating hours, OH	8000 h/year	
Natural gas boiler efficiency, η_{NG}	0.85	
Cash discounting rate, i	5 %	
Lifetime, n	20	

The exergy efficiency η_{ex} accounts for the exergy of the streams and is defined by Eq. (12) [23] (Zühlsdorf et al., 2018) considering a dead state at conditions of $T_o = 15\ ^\circ C$ and $p_o = 1$ bar.

$$\eta_{ex} = \frac{\dot{X}_{sink,out} - \dot{X}_{sink,in}}{\dot{X}_{source,in} - \dot{X}_{source,out} + \dot{W}_1 + \dot{W}_2 + \dot{W}_3} \tag{12}$$

The exergy of a stream, $\dot{X}$, is defined as the maximum work that can be obtained from a stream while it is brought from the initial state into thermodynamic equilibrium with the environment, as determined by Eq. (13):

$$\dot{X} = \dot{m}(h - h_o - T_o(s - s_o)) \tag{13}$$

where h and s are the specific enthalpy and specific entropy of the stream at the initial state and h_o and s_o are the specific enthalpy and specific entropy at the dead state.

3.4. Economic evaluation

To evaluate the economic performance, the investment cost and the annual cash flows must be calculated. The total cost of investment, TCI, includes the cost for equipment, piping, startup, working capital, and other expenses, and was estimated to be 400 % of the purchased equipment cost (PEC) of the compressors and heat exchangers [23] (Zühlsdorf et al., 2018). The cost for acquisition of compressors was determined based on the volumetric flow rate (Eq. (14)), while the cost for heat exchangers was calculated by their heat transfer area (Eq. (15)) [26] (Ommen et al., 2015).

$$PEC_{COM} = 34340.5\left(\frac{\dot{V}}{\eta_{vol,com}279.8}\right)^{0.73} \tag{14}$$

$$PEC_{HX} = 26860.0\left(\frac{A}{42}\right)^{0.8} \tag{15}$$

where $\eta_{vol,com}$ is the volumetric efficiency of a compressor and estimated by Eq. (16) [27] (Dincer, 2017):

$$\eta_{vol,com} = 0.06\left(1 - \frac{\nu_{in}}{\nu_{out}}\right) \tag{16}$$

The heat transfer areas of each control volume of the heat exchangers were determined using constant heat transfer coefficients (Table 2) and logarithmic mean temperature differences. The heat transfer area of the heat exchanger was then determined from the total area of all control volumes.

The assumed annual cash flows included the cost of electricity consumption, CF_{el}, (Eq. (17)) and the income from the supply of heat, CF_{supply}. In this study, the heat pump was considered to replace a natural gas boiler, and CF_{supply} was calculated from the reduction in annual

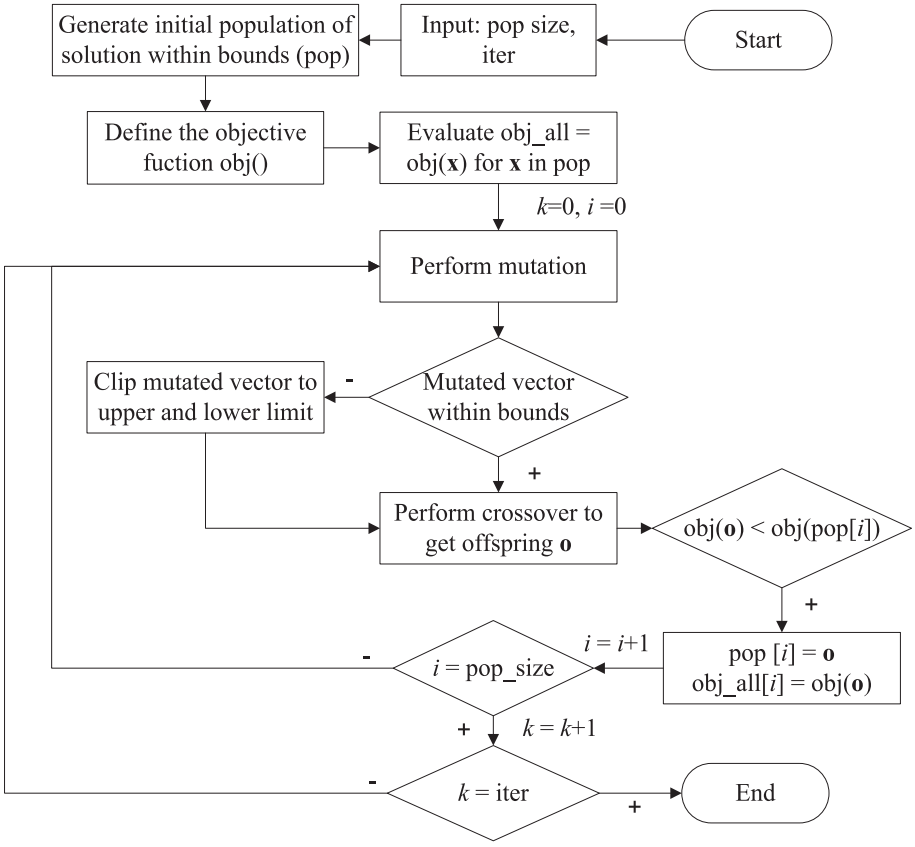

Fig. 3. Differential evolution algorithm.

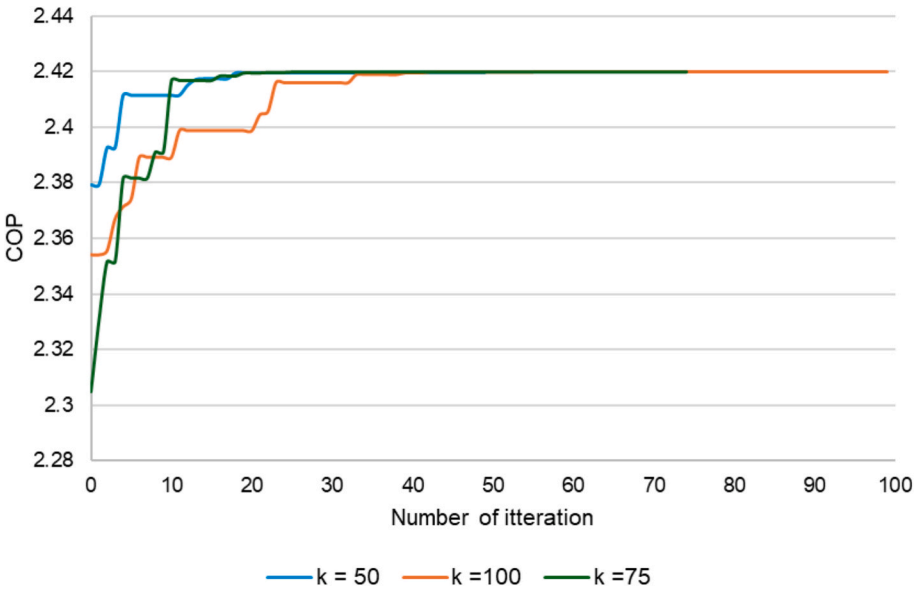

Fig. 4. The optimal COP of the cascade HTHP (TC = Acetone, BC = Neopentane) across iterations with the number of iteration of DE algorithm (*k*) set to 50, 75 and 100 iterations.

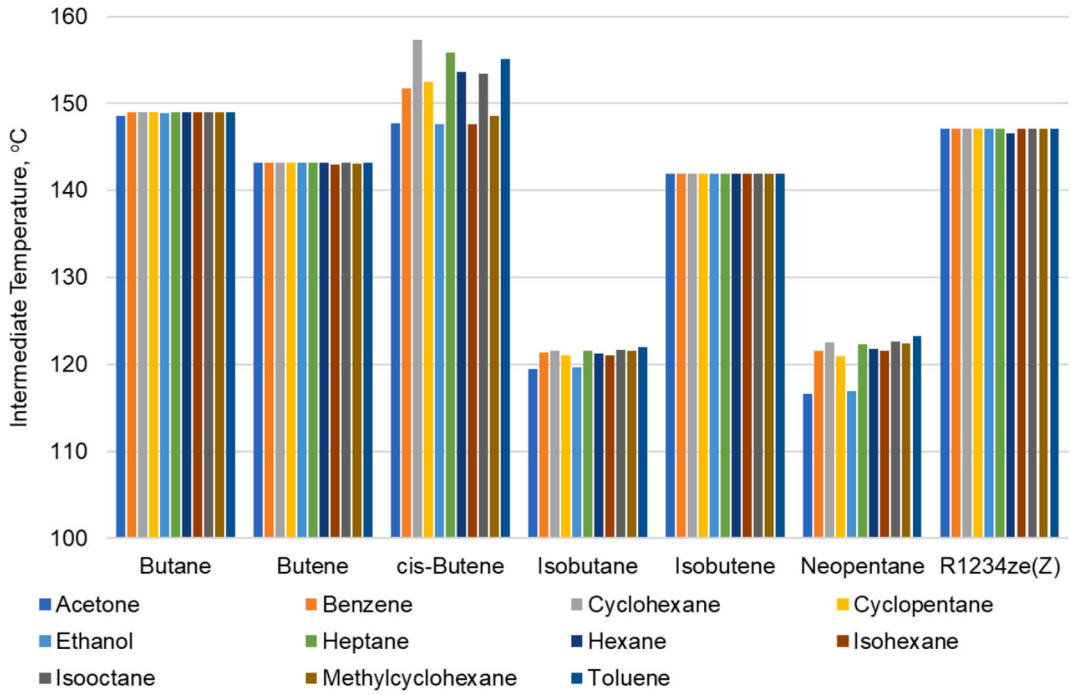

Fig. 5. Optimal intermediate temperature of the cascade heat pump for all refrigerant pairs (BC refrigerant listed on x-axis label with paired TC indicated by the legend).

natural gas consumption (Eq. (18)). The annual cash flow relating to the heat source CF_{source} was assumed to be zero as the heat source was obtained by recycling the exhausted heat of the spray dryer (Fig. 1). All parameters for economic analysis are summarized in Table 3.

$$CF_{el} = (c_{el} + E_{el} \cdot c_{carbon}) \cdot OH \cdot \sum \dot{W} \tag{17}$$

$$CF_{\text{supply}} = (c_{NG} + E_{NG} \cdot c_{carbon}) \cdot OH \cdot \frac{\dot{Q}_{\text{sink}}}{\eta_{NG}} \tag{18}$$

To compare annual cash flows and one-off costs, the capital recovery factor *CRF* (Eq. (19)) must be used. *CRF* was determined by a discounting rate *i*. The selection of discounting rate considers the risk of an investment; the greater the risk of the investment, the higher the rate should be. In this paper, *i* was selected as 5 % following [23] Zühlsdorf et al. (2018):

$$CRF = \frac{i(1+i)^n}{(1+i)^n - 1} \tag{19}$$

Three different criteria have been used for the economic performance: the net present value *NPV*, the payback time *PBT* and the specific cost of heat c_h. The *NPV* describes the value of the investment over its entire lifetime at the time of investment by accounting for investment cost and

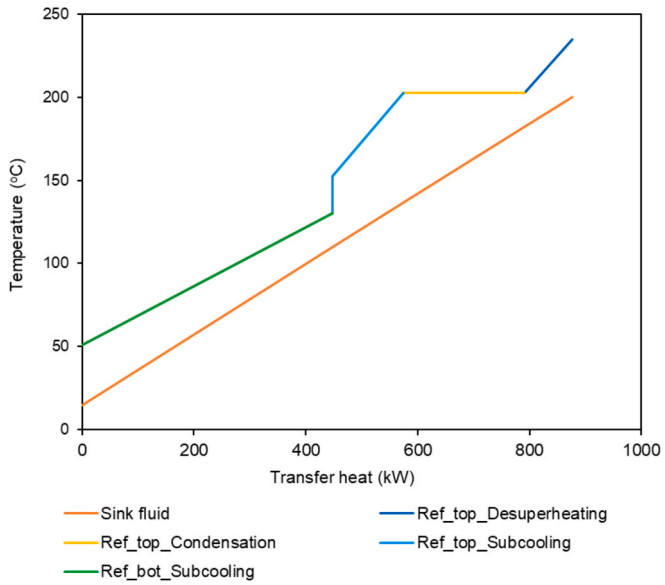

Fig. 6. Temperature −heat diagram of Acetone (TC)-Isobutane (BC) when T_{inter} increased beyond the optimized point.

annual cash flows.

$$NPV = -TCI + \frac{CF_{suply} - CF_{el}}{CRF} \tag{20}$$

The *PBT* determines the number of years required to compensate the initial investment:

$$PBT = \frac{TCI}{CF_{suply} - CF_{el}} \tag{21}$$

And the specific cost of heat c_h relates the annual equivalent of the *TCI* and the annual electricity consumption to the annual heat supplied:

$$c_h = \frac{TCI \cdot CRF + CF_{el}}{OH \cdot \dot{Q}_{sink}} \tag{22}$$

3.5. Optimization algorithm

In the cascade HTHP model, for each refrigerant combination evaluated, the intermediate temperature (T_{inter}), the increase in superheating temperature over IHX1 and IHX2 (ΔT_{SH1}, ΔT_{SH2}) and the vapor quality of the BC refrigerant entering HX3 (x_5) can be varied for optimization. Changing these variables has significant influence on the energy performance of the system. In this study, the differential evolution (DE) method was employed to obtain the best combination of these variables to maximize the COP of the cascade HTHP as it is capable of handling complex, multi-variable, non-convex problems typical of thermodynamic systems. Unlike gradient-based methods, DE (Fig. 3) performs a population-based global search, reducing the risk of being trapped in local optima, and increasing the likelihood of finding the true optimum. Its robustness, ease of implementation, and suitability for noisy or computationally expensive objective functions make it especially effective for simulation-based heat pump optimization tasks.

Similar to other direct search approaches, such as generic algorithms, the DE starts with an initial population (pop) of candidate solutions. These candidate solutions are iteratively improved by introducing mutation into the population (Eq. (23)), and retaining the fittest candidate solutions that yield a lower objective function value [31] (Kumar et al., 2022).

$$\mathbf{m} = \mathbf{x}_{r1} + F(\mathbf{x}_{r2} - \mathbf{x}_{r3}) \tag{23}$$

where F is the scale factor for mutation, $r_1 \neq r_2 \neq r_3$ are the indices indicating distinct and randomly selected individuals from the population.

DE algorithm used binominal crossover (Eq. (24)) which exchanges elements of n-dimensional parent vectors $\mathbf{x} = [x_1,\ldots, x_n]$ and mutated vector $\mathbf{m} = [m_1,\ldots, m_n]$ to create an offspring vector $\mathbf{o} = [o_1, \ldots, o_n]$

$$o_j = \begin{cases} m_j \text{ if } \text{rand}(0,1) \leq C_r \\ x_j \text{ otherwise} \end{cases} \text{ for } j = 1,\ldots,n \tag{24}$$

where C_r is the crossover rate for recombination.

For each refrigerant pair, the COP of the cascade HTHP model was estimated for every combination of T_{inter}, ΔT_{SH1}, ΔT_{SH2} and x_5. The negative value of COP was used as the objective function since the DE algorithm aims to find the minimum value of the object function. In the optimisation study, T_{inter} was limited by the critical temperature of the

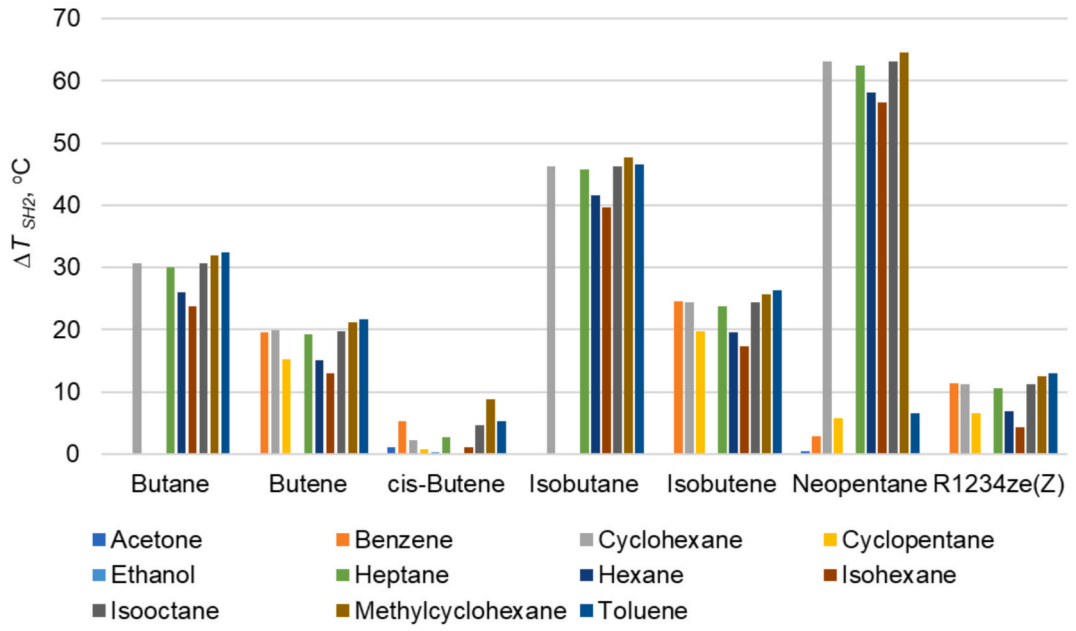

Fig. 7. Optimal superheated temperature across the IHX2.

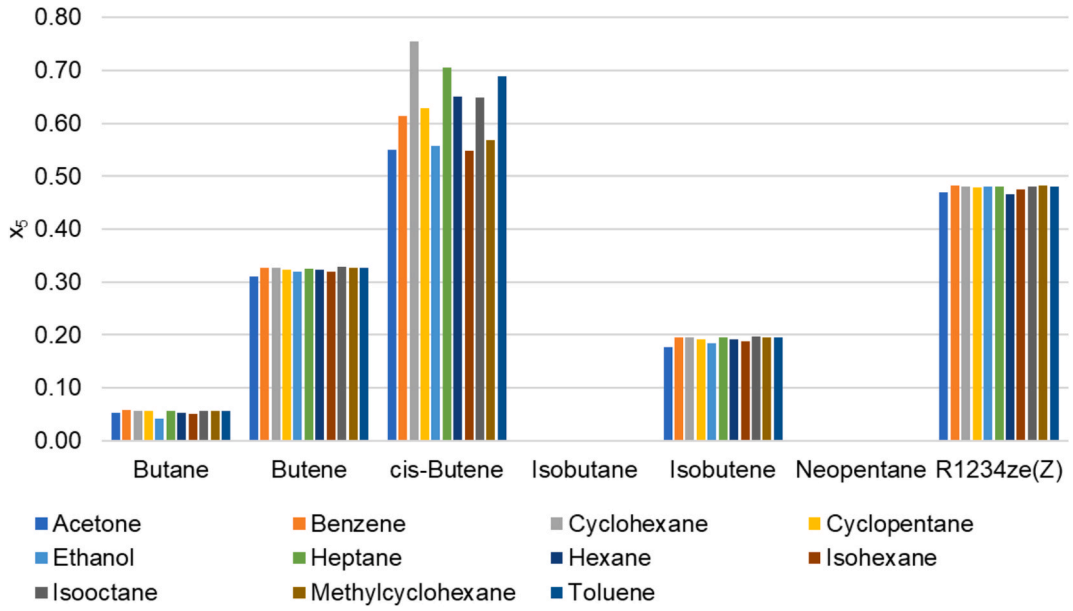

Fig. 8. Optimal vapor quality of BC refrigerant entering IHX3.

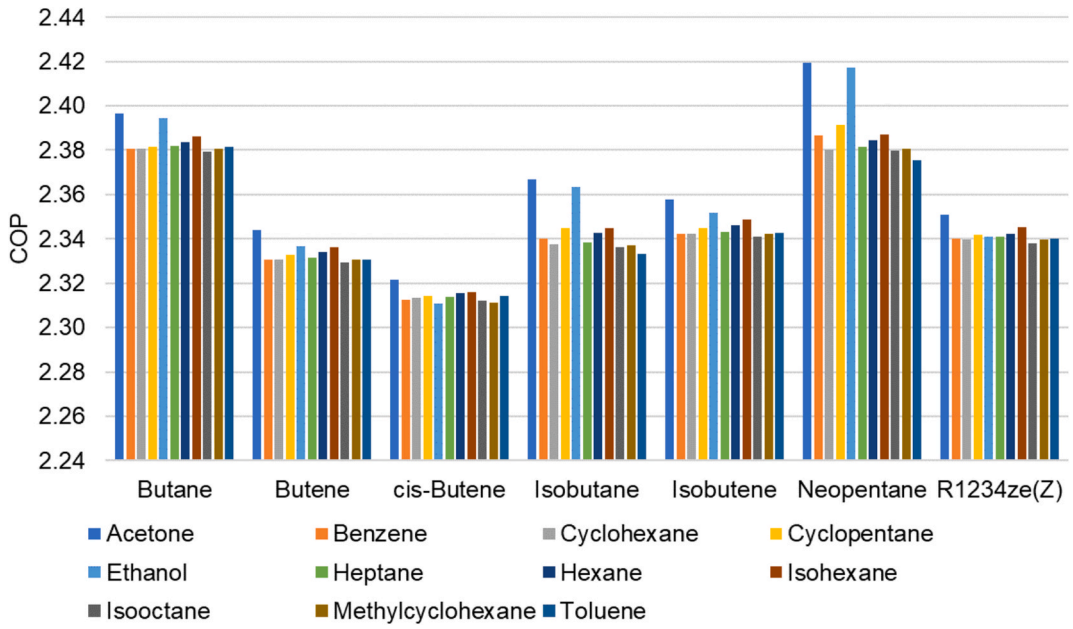

Fig. 9. Optimized COP of the cascade HTHP for all refrigerant pairs.

BC minus 3 °C to ensure the subcritical condition of the BC. The ΔT_{SH1}, ΔT_{SH2} ranged from 0 °C to 100 °C, while x_5 ranged from 0 to 1. The DE parameters – scaling factor F and crossover rate C_r were set to 0.5 and 0.7, respectively while the population size was set to 30.

The convergence behavior was monitored by tracking the best COP value across iterations. As shown in Fig. 4, most of the improvement occurred within the first 30 iterations, with only marginal gains observed thereafter, indicating that the solution had effectively stabilized well before reaching the 50th iteration.

The time required for each DE run depended on the complexity of the simulation model and the number of iterations. On average, the simulation times for 50, 75 and 100 iterations were 20 min, 30 min and 40 min, respectively on a DELL XPS (Intel i7, 2 × 2.59 GHz, 32 GB RAM), with run time being dominated by model evaluation rather than algorithm overhead. The number of iterations was set to 50 since it was sufficient to identify the optimum (Fig. 4).

To assess the reliability and quality of the obtained solution, the DE optimization was repeated 5 times using identical algorithm settings (F = 0.5, Cr = 0.7, population size = 30 and number of iteration = 50) with different random initial populations. The final optimal COP values showed minimal variation with the standard deviation of 2.0×10^{-7} suggesting that the DE consistently converged to the same region of the solution space. This repeatability, combined with the convergence after the first 30 iterations, provides strong evidence that the algorithm identified a global or near-global optimum under the given parameter settings.

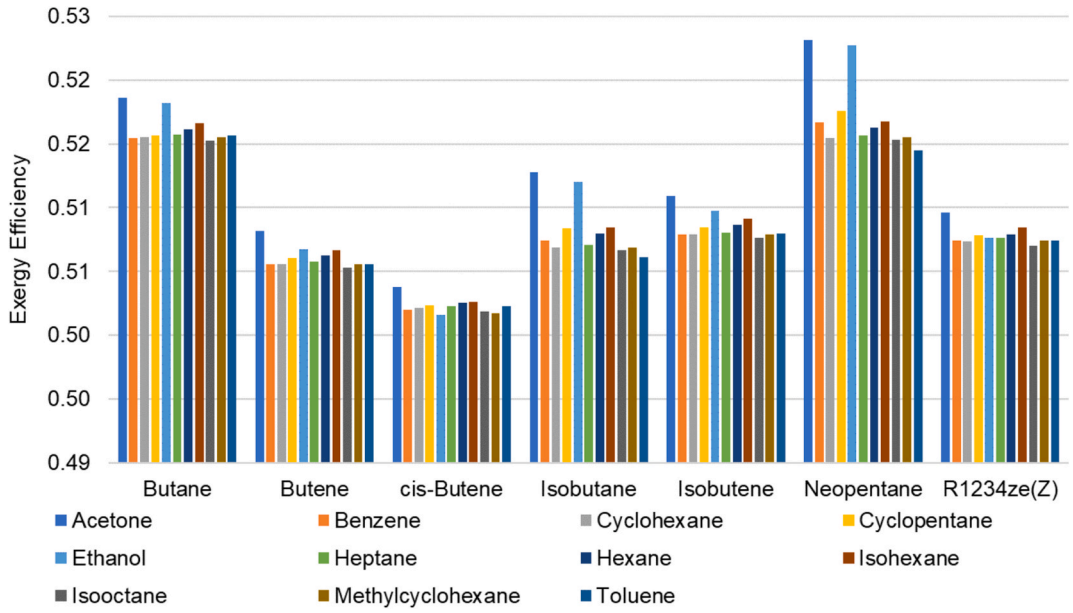

Fig. 10. Optimized exergy efficiency of the cascade HTHP for all refrigerant pairs.

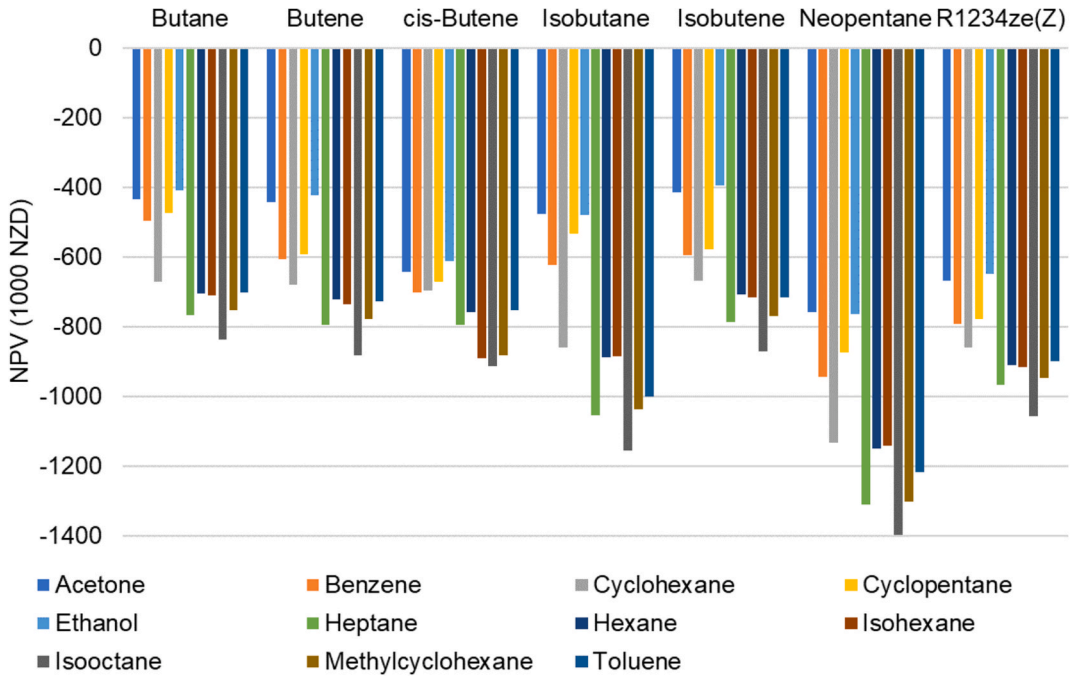

Fig. 11. NPV value of the cascade HTHP for all refrigerant pairs.

4. Results and discussion

4.1. Optimized configuration of the cascade cycle

The optimum intermediate temperature (T_{inter}) for all tested refrigerant pairs is shown in Fig. 5. The optimum value of the T_{inter} typically depends more heavily on the BC refrigerant than the TC refrigerant. Isobutane and neopentane had optimum intermediate temperatures around 120 °C, while the other BC refrigerants achieved higher values approaching the upper limit of T_{inter} (defined as 3 °C less than the critical temperature of BC in order to maintain subcritical operation of the cycle). This can be attributed to the fact that, for all BC refrigerants except isobutane and neopentane, the pinch point of HX3 consistently occurred at the sink fluid inlet (point 6). Increasing the intermediate temperature would raise the sink fluid temperature at the outlet of HX3, or enhance the heat transfer to the sink fluid before entering the condenser, resulting in an increased COP. In contrast, when isobutane and neopentane were used as BC refrigerant, the pinch point of HX3 shifted from the sink fluid inlet (point 6) to the sink fluid outlet (point 5) as T_{inter} increased beyond the optimized point. Beyond this point, further increases in the intermediate temperature would elevate the refrigerant temperature leaving HX3; thereby increasing temperature profile mismatch between refrigerant and the heat sink fluid at the HX3 (Fig. 6) and consequently decreasing the COP.

Fig. 7 illustrates that the superheated temperature across IHX2 (ΔT_{SH2}) depends on both BC refrigerant and TC refrigerant, and it tends

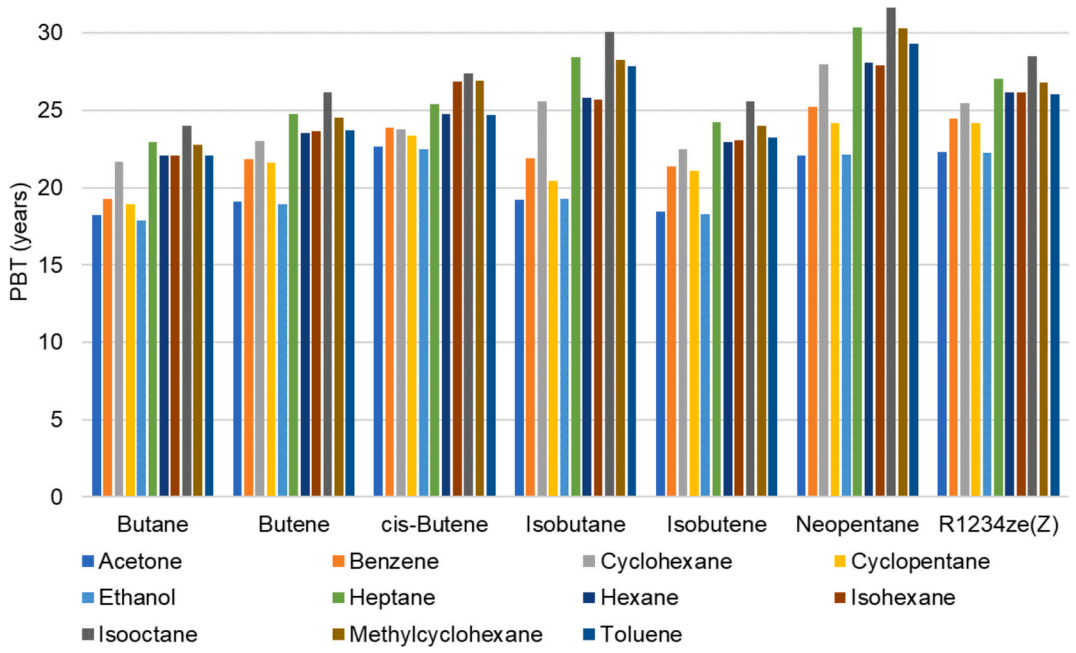

Fig. 12. PBT of the cascade HTHP for all refrigerant pairs.

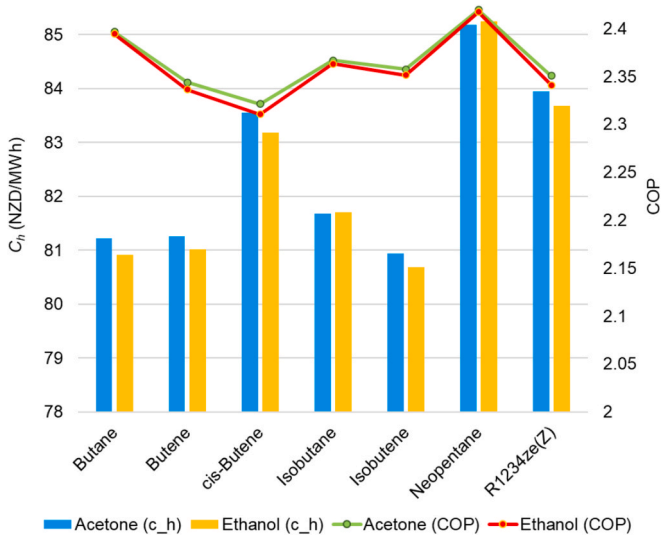

Fig. 13. Specific cost of heat (clustered columns) and COP (lines with markers) of the cascade HTHP using acetone and ethanol as the TC refrigerant and different BC refrigerants.

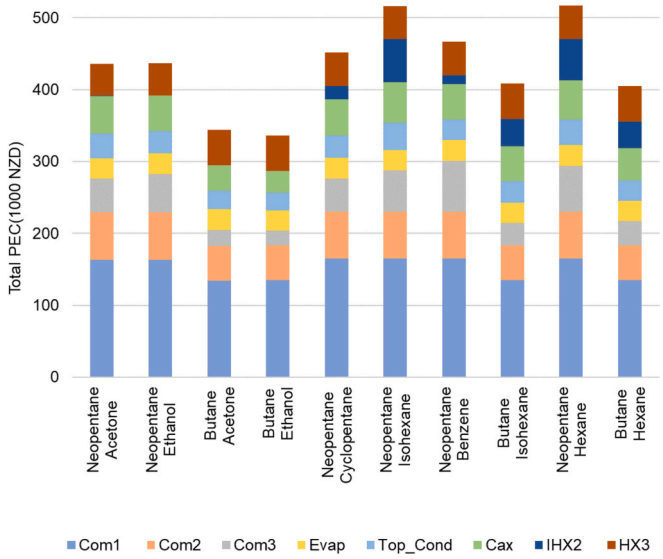

Fig. 14. Equipment purchase cost of heat pumps using the ten refrigerant pairs having highest COP.

to be high when T_{inter} is low and vice versa. Since the temperature of the hot liquid TC refrigerant entering IHX2 is limited by the critical temperature of the TC refrigerant ($T_{crit,top}$) in order to maintain subcritical operation, the temperature of the superheated vapor leaving IHX2 is also constrained to $T_{crit,top}$ minus $\Delta T_{\text{pinch,IHX}}$. Therefore, ΔT_{SH2} will depend on the temperature of TC refrigerant entering the IHX2 which in turn is limited by the temperature of the BC refrigerant entering the Cascade HX (*T4*). When T_{inter} (condensing temperature of BC) is low as in the case of isobutane and neopentane, the corresponding condensing pressure is also low, resulting in a low *T4*. Consequently, ΔT_{SH2} becomes relatively high. Conversely, when T_{inter} is high as in the case of butane, butene, *cis*-butane, isobutene and R1234ze(Z) *T4* is higher, leading to a lower ΔT_{SH2}.

The optimization results also indicated that the optimum vapor temperature difference across the IHX1 was zero for all tested refrigerant pairs. This can be explained by the fact that removing IHX1 allows the BC refrigerant to be reduced to the heat sink fluid inlet temperature plus $\Delta T_{\text{pinch,sink}}$. Consequently, it maximizes the utilization of the condensing heat of the BC to preheat the sink inlet through HX3 and improves the COP of the system.

The optimum vapor quality of BC refrigerant entering HX3 (x_5) is shown in Fig. 8. The value of x_5 depends solely on the BC refrigerant.

Table 4
The optimal COP of the cascade HTHP (TC = Acetone, BC = Neopentane) at with different random initial population of DE algorithm (F = 0.5, Cr = 0.7, population size = 30 and number of iteration = 50).

Trial	1	2	3	4	5	Standard deviation
Optimal COP	2.42	2.42	2.42	2.42	2.42	2.0E-07

Table 5
Summary of key thermodynamic performance for ten best-performing refrigerant pairs.

TC Refrigerant	BC Refrigerant	COP	η_{ex}	m_{bot}(kg/s)	m_{top}(kg/s)	$V_{suc,1}$ (m^3/h)	$V_{suc,2}$ (m^3/h)	$V_{suc,3}$ (m^3/h)	$P_{mid,bot}$ /$P_{evap,bot}$(bar/bar)	$P_{cond,bot}$ /$P_{mid,bot}$(bar/bar)	$P_{cond,top}$ /$P_{evap,top}$(bar/bar)
Acetone	Neopentane	2.42	0.52	1.67	0.86	1999.1	552.9	293.8	4.0/1.0	15.3/4.0	30.5/5.2
Ethanol	Neopentane	2.42	0.52	1.67	0.47	1999.2	551.4	319.3	4.0/1.0	15.4/4.0	30.9/3.5
Acetone	Butane	2.40	0.52	1.40	0.74	1438.1	322.6	134.2	7.3/1.5	35.9/7.3	29.9/10.5
Ethanol	Butane	2.39	0.52	1.40	0.41	1438.1	321.7	119.1	7.3/1.5	36.1/7.3	33.0/8.8
Cyclopentane	Neopentane	2.39	0.52	1.67	1.11	1999.7	532.6	277.3	4.1/1.0	16.5/4.1	33.3/6.2
Isohexane	Neopentane	2.39	0.52	1.67	1.54	2000.4	529.6	469.6	4.2/1.0	16.7/4.2	16.4/4.8
Benzene	Neopentane	2.39	0.52	1.67	0.98	1999.8	529.5	497.8	4.2/1.0	16.7/4.2	18.9/2.9
Isohexane	Butane	2.39	0.52	1.40	1.31	1438.2	321.6	219.5	7.3/1.5	36.1/7.3	19.7/8.4
Hexane	Neopentane	2.38	0.52	1.67	1.41	1999.8	528.2	535.7	4.2/1.0	16.8/4.2	14.6/3.9
Hexane	Butane	2.38	0.52	1.40	1.19	1438.2	321.6	245.4	7.3/1.5	36.1/7.3	17.5/7.0

Table 6
The optimal state points of the cascade refrigeration cycle when using acetone/neopentane as refrigerants.

Point	P (Mpa)	h(kJ/kg)	T(°C)	s(kJ/kgK)
1	0.1	359.0	35.0	1.3
2	0.1	359.0	35.0	1.3
3	0.40	426	76.2	1.3
4	1.5	493.7	124.1	1.4
5	1.5	277.5	116.6	0.8
6	1.5	59.4	35.0	0.2
7	1.5	59.4	35.0	0.2
8	0.1	59.4	10.0	0.2
9	0.52	579.1	121.1	1.5
10	0.52	579.9	121.5	1.5
11	3.05	700.6	227.8	1.6
12	3.05	161.8	124.5	0.4
13	3.05	161.0	124.2	0.4
14	0.52	161.0	113.6	0.4

While the cascade cycle using isobutane and neopentane as the BC refrigerant achieved the highest COP when these refrigerants entered HX3 as saturated liquid ($x_5 = 0$), the optimal value of x_5 when butane, butene, *cis*-butene, isobutane, and R1234ze(Z) were used as the BC refrigerant ranged from 0.05 to 0.7.

Figs. 9 and 10 present the optimized COP and the optimized exergy efficiency of the cascade HTHP respectively. The proposed cascade system achieved a COP higher than 2.3 and an exergy efficiency higher than 50 % for all refrigerant pairs for an output temperature of 200 °C. The heat pump performed best when butane or neopentane were used as BC refrigerants and acetone or ethanol were used as TC refrigerants.

Table 5 summarizes the relevant performance indicators for the best refrigerant pairs. Among the top ten refrigerant pairs, the highest COP of 2.42 was obtained with acetone/neopentane and ethanol/neopentane, followed by acetone/butane and ethanol/butane with COPs of 2.40 and 2.39, respectively. The exergy efficiency η_{ex} of the cascade HTHP for all refrigerant pairs listed in Table 5 was 52 %. While the thermodynamic performance of the cascade HTHP using neopentane as the BC refrigerant was slightly better than the system using butane, it had higher suction volumes incurring a higher investment cost. The optimal state points of the cascade refrigeration cycle when using acetone/neopentane as the TC/BC refrigerant is shown in Table 6.

4.2. Economic analysis

Figs. 11 and 12 provide an overview of the NPV value and PBT of the cascade HTHP. For the spray dryer case study using current prices, the heat pump was outperformed by natural gas based system which was illustrated by the negative values of NPV for all tested refrigerant pairs, which indicates that the relative prices of natural gas and electricity need to change in order for the heat pump option to be economical. Nonetheless, the results are useful for comparisons between the different refrigerant pairings.

The cascade HTHP achieved a higher NPV value and a faster PBT when acetone and ethanol were used as the TC refrigerant. This demonstrates the advantages of utilizing acetone and ethanol as TC refrigerants, not only in terms of thermodynamic performance but also economic performance. On the other hand, the heat pump showed worst economic performance in terms of NPV value and PBT when neopentane was used as the BC refrigerant.

Fig. 13 presents the comparison of specific cost of heat c_h and COP of the cascade HTHP using acetone and ethanol as the TC refrigerant and different BC refrigerants. The performances of the heat pump were nearly identical when acetone and ethanol were used as the TC refrigerants. Using butane as the BC refrigerant, the heat pump exhibited comparatively good performance in both thermodynamic and economic aspects, while the heat pump using Neopentane as the BC refrigerant achieved good thermodynamic performance but did not fare as well economically.

Table 7 summarizes the economic performance of the refrigerant pairs with the ten highest COPs. It is worth noting that the total capital investment per kW of heat (TCI_{spec}) of a heat pump using butane as BC refrigerant was approximately NZD 500 cheaper than the heat pump using neopentane as BC refrigerant, despite having a similar COP. This difference resulted in a lower NPV value for the neopentane heat pump, as well as higher PBT and c_h values compared to the butane heat pump.

Table 7
The economic performance of ten refrigerant pairs that had highest COP.

TC Refrigerant	BC Refrigerant	COP	TCI_{spec}(NZD/kW)	NPV(1000 NZD)	PBT(years)	c_h(NZD/MWh)
Acetone	Neopentane	2.42	2106	−759	22.1	85.19
Ethanol	Neopentane	2.42	2106	−764	22.2	85.24
Acetone	Butane	2.40	1650	−435	18.2	81.22
Ethanol	Butane	2.39	1613	−409	17.9	80.91
Cyclopentane	Neopentane	2.39	2162	−875	24.2	86.50
Isohexane	Neopentane	2.39	2470	−1143	27.9	89.71
Benzene	Neopentane	2.39	2231	−944	25.2	87.32
Isohexane	Butane	2.39	1952	−712	22.1	84.54
Hexane	Neopentane	2.38	2471	−1151	28.1	89.79
Hexane	Butane	2.38	1937	−705	22.0	84.45

Table 8
Thermodynamic and economic performance of cascade HTHP at design operating condition (bold) and off design conditions.

TC/BC Refrigerant	$T_{evap,bot}$	5 °C					10 °C				15 °C		
	$T_{sink,out}$	180 °C	190 °C	200 °C	210 °C	180 °C	190 °C	200 °C	210 °C	180 °C	190 °C	200 °C	210 °C
	COP	2.38	2.34	2.30	2.26	2.49	2.44	**2.40**	2.35	2.60	2.55	2.50	2.44
	η_{ex}	0.48	0.49	0.51	0.52	0.49	0.51	**0.52**	0.53	0.51	0.52	0.53	0.54
Acetone/	*NPV*, 1000NZD	−499	−615	−738	−858	−194	−313	**−435**	−571	73	−42	−171	−330
Butane	*PBT*, years	19.2	21.7	24.9	28.9	14.6	16.3	**18.2**	20.8	11.8	12.9	14.3	16.4
	COP	2.38	2.34	2.30	2.26	2.49	2.44	**2.39**	2.35	2.60	2.55	2.50	2.44
Ethanol/	η_{ex}	0.48	0.49	0.50	0.52	0.49	0.51	**0.52**	0.53	0.51	0.52	0.53	0.54
Butane	*NPV*, 1000NZD	−474	−595	−715	−833	−175	−292	**−409**	−548	92	−22	−150	−310
	PBT, years	19.0	21.5	24.7	28.7	14.4	16.0	**17.9**	20.6	11.6	12.7	14.1	16.2
	COP	2.48	2.42	2.35	2.27	2.59	2.51	**2.42**	2.33	2.62	2.55	2.49	2.41
Acetone/	η_{ex}	0.50	0.51	0.51	0.52	0.51	0.52	**0.52**	0.53	0.51	0.52	0.53	0.54
Neopentane	*NPV*, 1000NZD	−630	−780	−986	−1258	−333	−512	**−759**	−1066	−303	−431	−585	−734
	PBT, years	19.6	22.3	27.1	35.8	15.7	18.0	**22.1**	28.8	15.3	16.8	19.0	21.9
	COP	2.48	2.42	2.35	2.27	2.59	2.51	**2.42**	2.33	2.59	2.53	2.47	2.40
Ethanol/	η_{ex}	0.50	0.51	0.51	0.52	0.51	0.52	**0.52**	0.52	0.50	0.52	0.53	0.53
Neopentane	*NPV*, 1000NZD	−616	−764	−976	−1286	−313	−498	**−764**	−1183	−336	−401	−505	−746
	PBT, years	19.4	22.1	27.0	36.6	15.5	17.9	**22.2**	30.9	15.8	16.7	18.3	22.2

The highest estimated specific total investment cost was for the hexane/neopentane pairing at 2471 NZD/kW, while the lowest specific total investment cost was for the ethanol/butane pairing at 1613 NZD/kW.

The breakdown of the purchase equipment cost for heat pump using top ten refrigerant pairs is presented in Fig. 14. Taking approximately 60 % of the total purchase equipment cost, the compressors comprised the dominant expense, rather than the heat exchangers. Compressor 1 was identified as the most expensive component, while the cascade heat exchanger was the costliest among the heat exchangers. The higher investment cost of the neopentane heat pumps can be attributed to the high compressors cost, resulting from their higher suction volumes compared to butane heat pumps (as indicated in Table 4).

4.3. Off-design analysis

In the off-design analysis, it was assumed that the hot air temperature entering the spray dryer system could vary from 180 °C to 210 °C, while the bottom cycle evaporation temperature could be between 5 °C and 15 °C. Table 8 summarizes the thermodynamic and economic performance of cascade HTHP with acetone and ethanol as TC refrigerants and butane and neopentane as BC refrigerants under different operating conditions.

The COP of the heat pump decreases when the sink outlet temperature increases and the evaporation temperature decreases. In most cases, the heat pump using Neopentane as the BC refrigerant has a higher COP than the heat pump using butane except for the evaporation temperature of 15 °C. This can be explained by the fact that when the evaporation temperature of the heat pump using neopentane (which has a positive slope in the T-S diagram) as the BC refrigerant is high, the optimum condensing temperature of the bottom cycle is low and the optimum superheated temperature across IHX1 needs to be higher than zero to avoid wet compression at the outlet of Compressor 2. When the IHX1 is utilized to increase the superheated temperature of the refrigerant, it will increase the refrigerant temperature at the outlet of HX3. This, in combination with the low optimum condensing temperature of the bottom cycle, results in a decrease in the condensing heat of the bottom cycle that can be used to preheat the sink fluid inlet, and consequently, the COP will decrease.

The economic performance of the butane heat pump in terms of NPV, PBT consistently outperforms the neopentane heat pump. The thermodynamic and economic performance of the heat pump using acetone as TC refrigerant are similar to that of the heat pump using ethanol as TC refrigerant under off design conditions. The cascade HTHP became economical at the evaporation temperature of 15 °C and the supply air temperature of 180 °C if acetone/butane, or ethanol/butane were used as TC/BC refrigerants (NPV values of NZD 73,000 and NZD 92,000 respectively).

Among all operating conditions, the cascade HTHP achieves the best thermodynamic performance with the COP of 2.62 for evaporation temperature/sink outlet temperatures of 15 °C/180 °C when the TC/BC refrigerants were acetone/neopentane while the worst thermodynamic performance with the COP of 2.26 was obtained for evaporation temperature/ sink outlet temperatures of 5 °C/210 °C when the TC/BC refrigerants were acetone/butane or ethanol/butane.

4.4. Scope for future work

In its current form, the proposed cascade HTHP is not economically viable. However, future research and technological advancements have the potential to improve the performance of the system and make it economically viable. Key research areas include:

- Development of high-efficiency heat exchangers using materials capable of withstanding temperatures above 200 °C and high operating pressures.
- Optimization of pinch points and minimization of temperature differences to reduce exergy losses.
- Evaluation of oil-free, high-temperature compressors (e.g., turbo, scroll, or reciprocating types) specifically designed for high-temperature heat pump applications.
- Incorporation of real-time control strategies and thermal energy storage systems to support load balancing and peak shaving.
- Exploration of integration scenarios in industries that require process heat above 200 °C.
- Analysis of the retrofit potential of the HTHP in existing boiler-based systems.
- Investigation of integration of the cascade HTHP with industrial waste heat recovery systems or renewable electricity sources (e.g., solar PV) to enhance energy utilization and reduce dependency on expensive grid electricity.

5. Conclusions

This study simulated and optimized a novel cascade HTHP for spray dryer applications with a supply air temperature of 200 °C.

Only pure refrigerants with low GWP were considered, with seven refrigerants tested as BC refrigerants and eleven refrigerants tested as TC refrigerants. All refrigerant pairs achieved a COP higher than 2.3 and an exergy efficiency higher than 50 %. The best thermodynamic performance was observed when acetone or ethanol were used as TC refrigerants and butane and neopentane were used as BC refrigerants. The highest COP of 2.42 was obtained with acetone/neopentane and

ethanol/neopentane. While there was insignificant difference in terms of thermodynamic and economic performance between acetone and ethanol as TC refrigerants, the economic performance of butane as BC refrigerant was significantly better than that of neopentane. This can be attributed to the higher suction volumes when neopentane was used as the BC refrigerant.

The optimization results at the designed condition indicated that the heat pump achieves a higher COP when the IHX of bottom cycle was not used as it maximizes the condensation heat of the bottom cycle to pre-heat the sink inlet. The optimized intermediate temperature of the cascade cycle depends more on the BC refrigerant than the TC refrigerant.

Under off-design conditions with acetone and ethanol as the TC refrigerants, and butane and neopentane as the BC refrigerants, the cascade HTHP always achieves a COP higher than 2.26. A Positive NPV has been observed when acetone/butane, ethanol/butane were used as TC/BC refrigerants and the evaporation temperature and the supply air temperature were 15 °C and 180 °C, respectively.

CRediT authorship contribution statement

Duy K. Hoang: Writing – original draft, Validation, Project administration, Methodology, Investigation, Formal analysis, Data curation, Conceptualization. **Timothy G. Walmsley:** Writing – review & editing, Funding acquisition, Formal analysis, Conceptualization. **Don J. Cleland:** Writing – review & editing, Funding acquisition, Formal analysis. **Qun Chen:** Writing – review & editing, Formal analysis. **James K. Carson:** Writing – original draft, Supervision, Funding acquisition.

Declaration of competing interest

The authors declare that they have no known competing financial interests or personal relationships that could have appeared to influence the work reported in this paper.

Acknowledgements

This research was performed while author Hoang worked as a postdoctoral fellow at the Ahuora Centre for Smart Energy Systems, The University of Waikato and was supported by the program “Ahuora: Delivering sustainable industry through smart process heat decarbonization”, an Advanced Energy Technology Platform, funded by the New Zealand Ministry of Business, Innovation and Employment.

Data availability

Data will be made available on request.

REFERENCES

[1] MBIE, 2017. Process Heat in New Zealand–Overview https://www.mbie.govt.nz/assets/8c89799b73/process-heat-current-state-fact-sheet.pdf.
[2] P. Hall, Residual biomass fuel projections for New Zealand - Indicative availability by region and source, Scion Report, https://www.bioenergy.org.nz/documents/resource/Reports/Wood-residue-resources-report-2017_170824.pdf.
[3] C. Arpagaus, F. Bless, J. Schiffmann, S.S. Bertsch, Multi-temperature heat pumps: a literature review, Int. J. Refrig. 69 (2016) 437–465, https://doi.org/10.1016/jijrefrig.2016.05.014.
[4] S.T. Kim, R. Hegner, G. Özuylasi, P. Stathopoulos, E. Nicke, Performance analysis of high temperature heat pump cycle for industrial process. Performance Analysis of High Temperature Heat Pump Cycle for Industrial Process, 2021.
[5] J. Unterluggauer, V. Sulzgruber, C. Kroiss, J. Riedl, R. Jentsch, R. Willinger, Design for a heat pump with sink temperatures of 200 °C using a radial compressor, Energies 16 (13) (2023) 4916.
[6] K.-M. Adamson, T.G. Walmsley, J.K. Carson, Q. Chen, F. Schlosser, L. Kong, D. J. Cleland, High-temperature and transcritical heat pump cycles and advancements: a review, Renew. Sustain. Energy Rev. 167 (2022) 112798.
[7] A. Mota-Babiloni, C. Mateu-Royo, J. Navarro-Esbrí, F. Molés, M. Amat-Albuixech, Á. Barragán-Cervera, Optimisation of high-temperature heat pump cascades with internal heat exchangers using refrigerants with low global warming potential, Energy 165 (2018) (2018) 1248–1258.
[8] X. Li, Y. Zhang, X. Ma, N. Deng, Z. Jin, X. Yu, W. Li, Performance analysis of high-temperature water source cascade heat pump using BY3B/BY6 as refrigerants, Appl. Therm. Eng. 159 (2019) 113895.
[9] A. Uusitalo, T. Turunen-Saaresti, J. Honkatukia, J. Tiainen, A. Jaatinen-Värri, Numerical analysis of working fluids for large scale centrifugal compressor driven cascade heat pumps upgrading waste heat, Appl. Energy 269 (2020) (2020) 115056.
[10] Y. Dong, H. Yan, R. Wang, Significant thermal upgrade via cascade high temperature heat pump with low GWP working fluids, Renew. Sustain. Energy Rev. 190 (2024) 114072, https://doi.org/10.1016/j.rser.2023.114072.
[11] Y. Dong, R. Wang, When and how to use cascade high temperature heat pump—its multi-criteria evaluation, Energy Conv. Manag. 309 (2024) 118435, https://doi.org/10.1016/j.enconman.2024.118435.
[12] J. Song, J. Kim, S. Eom, J. Lee, Y. Chu, J. Kim, S. Choi, M. Choi, G. Choi, Y. Park, Study on the refrigerant interchangeability under extreme operating conditions of R1234yf heat pump systems for electric vehicles, Appl. Therm. Eng. 122789 (245) (2024), https://doi.org/10.1016/j.applthermaleng.2024.122789.
[13] T. Trevisan. European Parliament Approves Bans of HFCs and HFOs in Multiple Applications and HFC Phase Out by 2050 https://naturalrefrigerants.com/european-parliament-approves-bans-of-hfcs-and-hfos-in-multiple-applications-and-hfc-phase-out-by-2050.
[14] EU. Per- and polyfluoroalkyl substances (PFAS) https://echa.europa.eu/hot-topics/perfluoroalkyl-chemicals-pfas.
[15] X. Hu, C. Shi, Y. Liu, X. Fu, T. Ma, M. Jin, Advanced exergy and exergoeconomic analysis of cascade high-temperature heat pump system for recovery of low-temperature waste heat, Energies 17 (2024) 1027, https://doi.org/10.3390/en17051027.
[16] P. Ganesan, T.M. Eikevik, K. Hamid, R. Wang, H. Yan, Thermodynamic analysis of cascade high-temperature heat pump using new natural zeotropic refrigerant mixtures: R744/R600 and R744/R601, Int. J. Refrig 154 (2023) 215–230.
[17] S.M. Hosseinnia, H. Nesreddine, D. Monney, S. Poncet, Thermodynamic analysis of high temperature cascade heat pump with R718 (high stage) and six different low-GWP refrigerants (low stage), Case Stud. Therm. Eng. 53 (2024) 103812, https://doi.org/10.1016/j.csite.2023.103812.
[18] H. Zou, X. Li, M. Tang, J. Wu, C. Tian, D. Butrymowicz, Y. Ma, J. Wang, Temperature stage matching and experimental investigation of high-temperature cascade heat pump with vapor injection, Energy 212 (2020) 118734.
[19] H. Zou, X. Li, M. Tang, J. Wu, C. Tian, Optimization analysis and experimental investigation on high temperature cascade heat pump with vapor injection, in: International Conference on Applied Energy (ICAE 2019), Aug 2019.
[20] S. Dong, X. Meng, X. Hu, Z. Sun, H. Wang, Y. Luo, Investigation of cascade high temperature heat pump optimal design theory based on experiment supporting multi-objective optimization, Energy Conv. Manag. 267 (2022) 115873.
[21] T.G. Walmsley, M.R. Walmsley, M.J. Atkins, J.R. Neale, A.H. Tarighaleslami, Thermo-economic optimisation of industrial milk spray dryer exhaust to inlet air heat recovery, Energy 90 (2015) 95–104.
[22] E.W. Lemmon, I.H. Bell, M.L. Huber, M.O. McLinden, NIST Standard Reference Database 23: Reference Fluid Thermodynamic and Transport Properties-REFPROP, Version 10.0, in: National Institute of Standards and Technology, Standard Reference Data Program, Gaithersburg, 2018.
[23] B. Zühlsdorf, W. Meesenburg, T. Ommen, J. Thorsen, W.B. Markussen, B. Elmegaard, Improving the performance of booster heat pumps using zeotropic mixtures, Energy 154 (2018) 390–402.
[24] S. Fukuda, C. Kondou, N. Takata, S. Koyama, Low GWP refrigerants R1234ze(E) and R1234ze(Z) for high temperature heat pumps, Int. J. Refrig 40 (2014) 161–173.
[25] F.P. Incropera, D.P. DeWitt, T.L. Bergman, A.S. Lavine, Fundamentals of heat and mass transfer, 6 ed., Wiley, New York, 2007.
[26] T. Ommen, J.K. Jensen, W.B. Markussen, L. Reinholdt, B. Elmegaard, Technical and economic working domains of industrial heat pumps: Part 1–Single stage vapour compression heat pumps, Int. J. Refrig 55 (2015) 168–182.
[27] I. Dincer, I., *Refrigeration systems and applications*, John Wiley & Sons, 2017.
[28] MBIE, 2022, *Energy prices*. https://www.mbie.govt.nz/building-and-energy/energy-and-natural-resources/energy-statistics-and-modelling/energy-statistics/energy-prices/.
[29] MfE, 2022, Measuring emissions: A guide for organisations: 2022 summary of emission factors.
[30] Carbonnews, 2023. https://www.carbonnews.co.nz/.
[31] B.V. Kumar, D. Oliva, P.N. Suganthan, Differential Evolution: from Theory to Practice, Springer, 2022.